

## Contrast of 180° Domains of PbTiO<sub>3</sub> in an Electron Microscopic Image

BY MICHIOYOSHI TANAKA

Department of Physics, Faculty of Science, Tohoku University, Sendai, Japan

(Received 16 January 1974; accepted 27 July 1974)

The contrast of 180° domains of PbTiO<sub>3</sub> depends on temperature and is caused by differences in the intensity of the diffuse background. The thickness extinction fringes of 180° domains taken at different temperatures between room temperature and near the Curie temperature are qualitatively explained with the use of many-beam dynamical theory, in which different anomalous absorption factors are assumed for each case. The origin of the contrast is interpreted and discussed in terms of the difference in thermal diffuse scattering between the 180° domains.

### 1. Introduction

It has been reported that the ferroelectric 180° domains of BaTiO<sub>3</sub> (Tanaka & Honjo, 1964; Gevers, Blank & Amelinckx, 1966) are observed with a distinct contrast in the electron-microscopic image. Similar contrast has been observed in the cases of PbTiO<sub>3</sub>, KNbO<sub>3</sub> (Tanaka, Yatsushashi & Honjo, 1970) and LiNbO<sub>3</sub> (Wicks & Lewis, 1968), but previous detailed studies have been concentrated on BaTiO<sub>3</sub>.

It was revealed that the contrast of the 180° domains of BaTiO<sub>3</sub> is due to the failure of Friedel's law and that the failure in this case may be understood in terms of the many-beam dynamical theory (Tanaka & Honjo, 1964). Gevers, Blank & Amelinckx (1966) attempted a quantitative explanation of the contrast in terms of the two-beam dynamical theory. They found that the theoretical intensity ratio

$$\frac{|I_{002} - I_{00\bar{2}}|}{\frac{1}{2}(I_{002} + I_{00\bar{2}})} \simeq 0.4 \quad (\text{or } I_{00\bar{2}}/I_{002} \simeq 1.5)$$

by assuming the absorption potential to be 90° out of phase with the scattering potential. If this assumption holds, it can be concluded that anomalous transmission must not take place. It is, however, observed in the BaTiO<sub>3</sub> case. Tanaka & Honjo (1966) reported that the measured intensity ratio  $I_{002}/I_{00\bar{2}}$  becomes sometimes  $\sim 2.0$ . They analysed the thickness extinction fringes of adjacent 180° domains by Kohra & Watanabe's (1961) method, which is based upon two-beam theory and makes it possible to evaluate the values of the normal and anomalous absorption factors. From this analysis it was found that a theoretical treatment based on the two-beam theory is not adequate to interpret the observations. Tanaka & Honjo (1970) succeeded in explaining the characteristic difference between the 002 and 00 $\bar{2}$  thickness extinction fringes observed in adjacent 180° domains by using a nine-systematic-beam calculation. The calculation was made with phenomenological absorption factors which are not in phase with the scattering factors. This phase difference, however, has not been explained physically.

In order to know the main origin of the contrast for

these substances, the temperature dependence of the contrast observed in PbTiO<sub>3</sub> has been studied. PbTiO<sub>3</sub> is a favourable substance since it is tetragonal over a wide temperature range and its domains are very stable. Observations and analysis of the temperature dependence of the contrast are described in § 3(a) and the explanation of thickness-extinction fringes of adjacent 180° domains at room and high temperatures by many-beam dynamical theory using different absorption factors for each is given in § 3(b). The contrast, its temperature dependence and evaluated values of anomalous absorption factors are interpreted and discussed in terms of thermal diffuse scattering (TDS) in § 4.

### 2. Experimental

Thin-film specimens of PbTiO<sub>3</sub> were prepared by chemical polishing of single-crystal plates grown by the flux method. The plates were parallel to the 100 plane. Phosphoric acid was used at about 200°C as the polishing agent. The procedure of thin-specimen preparation was similar to that for BaTiO<sub>3</sub> (Tanaka & Honjo, 1964). At the polishing temperature, PbTiO<sub>3</sub> is tetragonal. Though it is known in general that the polishing rates for *a* and *c* domains are different, the effect of selective polishing was not observed in the present case. As the polishing rate for PbTiO<sub>3</sub> is smaller than that for BaTiO<sub>3</sub>, the thickness of the thin specimens was comparatively easily controlled. The observation of domains is easier than for BaTiO<sub>3</sub>, since the domains of PbTiO<sub>3</sub> do not move under normal electron irradiation. Carbon-film coating (Tanaka & Honjo, 1964) for eliminating the charging-up effect was not necessary. A JEM-7A with the commercial heating-tilting stage (A.H.G.) was used at the operating voltage, 100 kV.

### 3. Results

#### (a) Observation

Fig. 1 shows (a) the bright-field, (b) the 001 dark-field and (c) the 002 dark-field electron micrographs of the 180° domains of PbTiO<sub>3</sub> taken at room temperature, the

002 and 00 $\bar{2}$  reflexions being exactly excited for adjacent 180° domains. In the bright-field image, the thickness extinction fringes connect continuously at the domain boundary. No intensity difference is observed between the domains (Pogany & Turner, 1968). This ensures that there exists no misorientation between the domains. In the 001 dark-field image, a systematic shift of fringes is seen at the domain boundary owing to the failure of Friedel's law. This failure of Friedel's law is not explained by two-beam dynamical theory but must be explained by many-beam theory. According to two-beam theory, the fringes of adjacent 180° domains should not shift relative to each other but have different intensities, that is, the intensity of the fringe of one domain is stronger than that of the other domain (Tanaka & Honjo, 1966; Gevers *et al.*, 1966). In the 002 dark-field image extinction fringes connect continuously as in the case of the bright-field image. A slight intensity difference is observed between the two domains, so that the existence of 180° domains is observed in the extra contrast of the boundary region. This shows a remarkable difference from the result obtained for BaTiO<sub>3</sub>, in which the intensity difference between the adjacent domains is clearly seen even at room temperature (Tanaka & Honjo, 1964). Fig. 2 shows (a) the bright-field, (b) the 002 dark-field and (c) the 00 $\bar{2}$  dark-field electron micrographs taken at 200°C, where the 002 and 00 $\bar{2}$  reflexions were exactly excited. Thickness extinction fringes again connect smoothly at the domain boundaries. In the bright-field image (a), no contrast can be seen between adjacent domains, indicating no misorientation between the domains. In the dark-field images (b) and (c), distinct contrast appears and the contrast is reversed as the excited reflexion is reversed. Fig. 3 shows the temperature dependence of the ratio of the 002 and 00 $\bar{2}$  reflected intensities. The total intensity is divided into two parts, the peak and the background intensities, as shown schematically in Fig. 4. The ratios of the total, peak and background intensities of the 002 and 00 $\bar{2}$  reflexions are denoted by  $R_t$ ,  $R_p$  and  $R_b$  respectively. The value of  $R_p$  is slightly greater than 1.0 and is nearly constant. The ratio  $R_d$  changes greatly with the temperature of the specimen; that is, the value of  $R_b$  is very close to 1.0 at room temperature, becomes maximum at a certain temperature ( $\sim 300^\circ\text{C}$ ) and then decreases again. These ratios must be unity above 490°C, which is the Curie temperature ( $T_c$ ) of PbTiO<sub>3</sub>. The ratio  $R_t$  depends on temperature, but is closer to 1.0 than the ratio  $R_b$ , because the background intensity is smaller than the peak intensity at the present thickness. It must be emphasized that only the background intensity depends strongly on temperature. At high temperatures the 002 and 00 $\bar{2}$  fringes have nearly the same peak intensities but have different background intensities, which produce the contrast between the 180° domains. This behaviour is exactly the same as that observed for BaTiO<sub>3</sub> at room temperature (Tanaka & Honjo, 1966, 1970).

### (b) Calculations

The many-beam calculation was carried out by two methods, in neither of which is the perturbation method used. One is the method developed by Fujimoto (1959) in which the scattering matrix is expanded as a power series in the thickness; to improve the slowly convergent nature of the series, the manner of expansion was modified according to Niehrs (1959). The other is a diagonalization method by which a non-symmetric and complex matrix can be diagonalized. The computer program for this method is listed under the name of *ALLMAT* in the I.B.M. library.\* The agreement between the results calculated by these two methods was checked in advance.

The absorption factor of the 00 $l$  reflexion is expressed formally as

$$F'(\pm l) = F'_r(l) \pm iF'_i(l)$$

\* Share Program Library Agency, Cosmic Barrow Hall, Univ. of Georgia, Georgia 30601, U.S.A.

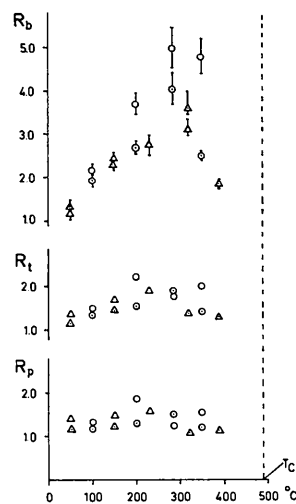


Fig. 3. The temperature dependence of the ratios of the 002 and 00 $\bar{2}$  reflected intensities obtained at the exact Bragg setting and at a fixed thickness.  $R_b$ ,  $R_t$  and  $R_p$  denote the ratios of background, total and peak intensities respectively, which are illustrated in Fig. 4. Each mark corresponds to a different measurement.

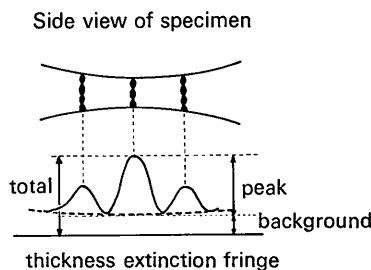


Fig. 4. Illustration of the definition of background, total and peak intensities.

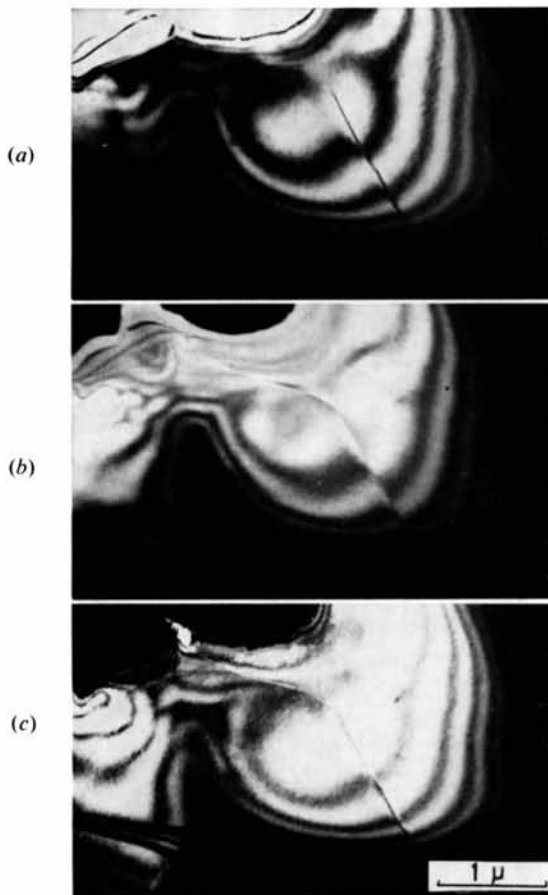


Fig. 1. (a) Bright-field, (b) 001 dark-field and (c) 002 dark-field micrographs of  $180^\circ$  domains of  $\text{PbTiO}_3$  taken at room temperature.

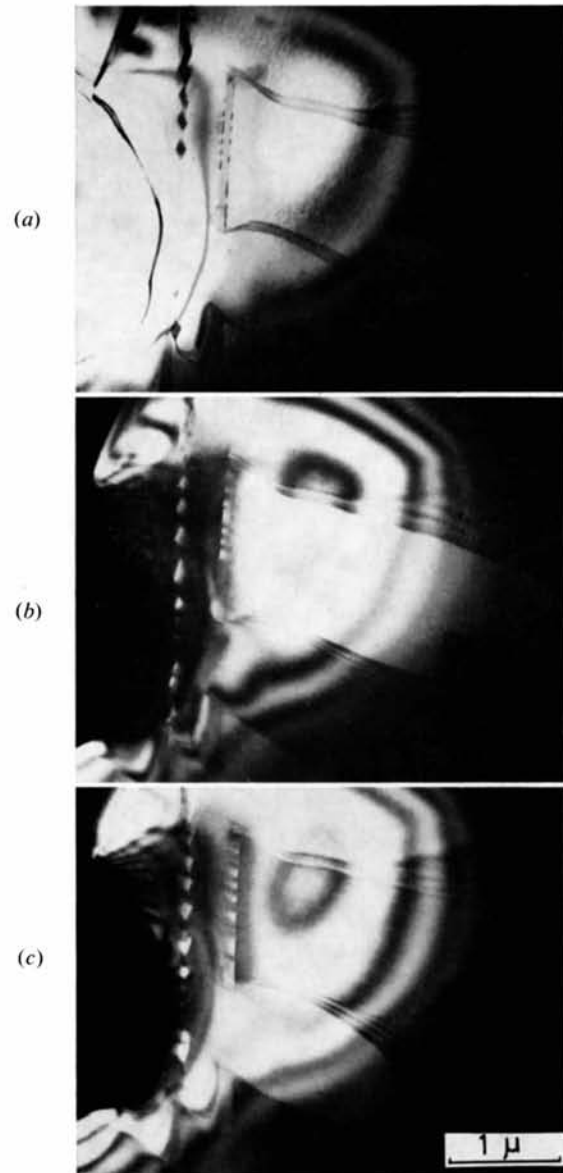


Fig. 2. (a) Bright-field, (b) 002 dark-field and (c)  $00\bar{2}$  dark-field micrographs of  $180^\circ$  domains of  $\text{PbTiO}_3$  taken at  $200^\circ\text{C}$ .

where  $F_r(l)$  and  $F_i(l)$  represent the real and imaginary parts. In the present case the values of these terms were so determined as to reproduce the experimental intensities under the appropriate assumption about scattering-angle dependence.

Fig. 5(a) and (b) shows the theoretical thickness extinction fringes of the  $\{001, 00\bar{1}\}$  and  $\{002, 00\bar{2}\}$  re-

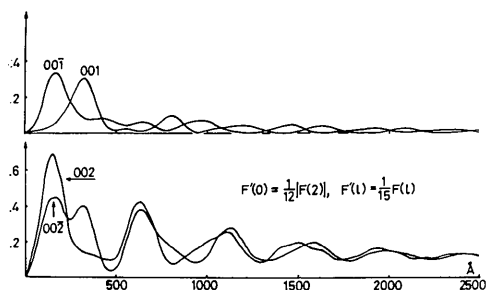


Fig. 5. Thickness extinction fringes of (a)  $\{001, 00\bar{1}\}$  and (b)  $\{002, 00\bar{2}\}$  reflexions of  $\text{PbTiO}_3$  obtained by nine-beam calculation. Proportionality is assumed between the crystal structure factor and the absorption factor.

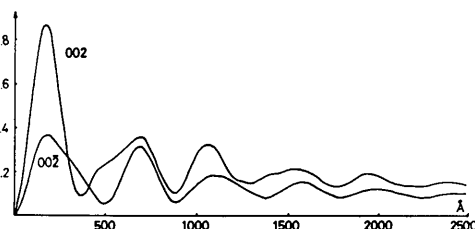


Fig. 6. Thickness extinction fringes of  $\{002, 00\bar{2}\}$  reflexions of  $\text{PbTiO}_3$  obtained by nine-beam calculation.  $F_r'(0) = \frac{1}{10} F_r(2)$ ,  $F_r'(l) = \frac{1}{10} F_r(l)$ ,  $F_i'(2l-1) = -\frac{1}{4} F_i(2)$ ,  $F_i'(2l) = -\frac{1}{8} F_i(2)$ .

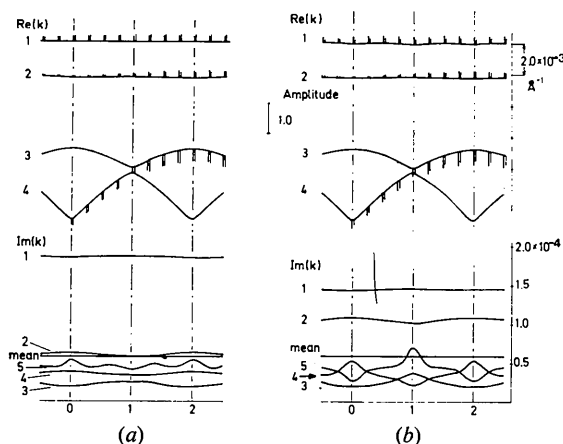


Fig. 7. Dispersion surface and associated amplitudes of  $\text{PbTiO}_3$ . The real parts of the branches are numbered from the top and the corresponding numbers are given for the imaginary parts. Thick and thin-line segments represent the amplitudes of the 002 and  $00\bar{2}$  reflexions. The segment attached upward (downward) on the branches indicates that the sign of the amplitude is positive (negative). The magnitude of the maximum amplitude ( $=1$ ) is shown between (a) and (b).  $F_r'(l) = \frac{1}{10} F_r(l)$ ,  $F_r'(0) = \frac{1}{10} F_r(2)$ , (a)  $F_i'(l) = \frac{1}{10} F_i(l)$ ; (b)  $F_i'(2l-1) = -\frac{1}{4} F_i(2)$ ,  $F_i'(2l) = -\frac{1}{8} F_i(2)$ .

flexions, respectively. The fringes were calculated with the nine-beam approximation for the  $\pm 002$  Bragg settings, where absorption factors were assumed to be  $F_r'(0) = \frac{1}{12} |F(2)|$  and  $F_r'(l) = \frac{1}{15} F_r(l)$  ( $l \neq 0$ ) (the proportional-type absorption). One can clearly see that the 001 and  $00\bar{1}$  fringes are shifted relative to each other by one half period at a thickness of more than 500 Å. The 002 and  $00\bar{2}$  fringes at the thick region have only a slight relative shift, with little difference between their peak intensities and no intensity difference between their background. Qualitatively, these results correspond well with the observation shown in Fig. 1. The complicated difference in the thin region may be difficult to observe. It is noted that the observed thickness extinction fringes at room temperature can be explained with the use of the proportional-type absorption factors usually postulated.

Crystal structure factors vary with temperature as a result of changes in the temperature factor, the lattice spacing and the relative positions of atoms in the unit cell. However, one cannot expect an increase of contrast from these changes, since the temperature factor more or less causes a reduction of the many-beam effect and the structural change causes a decrease in the deviation of the atoms from centrosymmetric positions. Consequently, the intensity difference between 002 and  $00\bar{2}$  thickness fringes at high temperatures should be interpreted as a result of a change in the absorption factors. However, the intensity difference was not reproduced by changing the value of the proportional factor between the crystal structure factor and the absorption factor. In order to reproduce the difference, computations were carried out, varying the type and values of absorption factors. Two types of absorption factors, the proportional-type and the  $\delta$ -type, were tested. The real part  $F_r'(l)$  and the imaginary part  $F_i'(l)$  were assumed to be able to be of different types. The values of  $F_r'(l)$  and  $F_i'(l)$  were varied independently. The case in which the sign of the odd-order factors  $F_i'(2l+1)$  is opposite to that of the even-order factors  $F_i'(2l)$  was also tested. Fig. 6 shows the best computed result. The absorption factors used are given in the figure. The properties, that the periodicity and phase of the fringes are the same, the background intensities different and the peak intensities nearly the same, are reproduced. The properties were not reproduced by the same type of absorption as used in the case of  $\text{BaTiO}_3$ .

Fig. 7 shows the dispersion surface and associated amplitudes of the 002 and  $00\bar{2}$  reflexions for the cases reproducing the thickness fringes at (a) room temperature and (b) high temperatures. The 002 and  $00\bar{2}$  amplitudes are depicted on the corresponding branches with the thick and thin-line segments respectively. The real parts of the eigenvalues are nearly unchanged between (a) and (b), but the imaginary parts change, corresponding to the change of the values of the absorption factors. The relative change of amplitude between (a) and (b) is larger on the first and third

branches than on the second branch. An explanation for the intensity difference between the 002 and 00 $\bar{2}$  thickness extinction fringes is given in terms of the dispersion surface and associated amplitudes. If a not very thin region is concerned, the contribution from the first branch can be ignored since it has large absorption, and only two branches remain. Thus, the periodicity of the two fringes is always the same. At room temperature the amplitude difference between the two reflexions is small. Therefore a slight intensity difference appears. On the other hand, at high temperatures the difference in the amplitudes between the reflexions is enhanced only on the third branch. The thickness fringe of one domain formed by the two waves which have a larger difference in their amplitudes (thick-line segments) has higher background than the fringe of the adjacent domain (thin-line segments).

#### 4. Discussion

From the fact that the contrast depends on temperature, it is clear that TDS plays an important role in the contrast phenomena. The observed thickness fringes at room and high temperatures were explained phenomenologically by many-beam calculations using different absorption factors for each. From the results the importance of the anomalous absorption for the contrast became evident.

However, the absorption factors obtained for the case of high temperatures are complicated and have large values. The factors cannot be understood without accepting that the positions where the absorption takes place are largely different from the positions of the atomic planes, as in the case of BaTiO<sub>3</sub>. This is difficult to understand physically. It should be noted that in the calculation the images were assumed to be formed only by elastically scattered electrons; in other words, the effect of TDS is assumed to appear through the anomalous absorption factors.

The absorption factors for BaTiO<sub>3</sub> obtained by convergent-beam electron diffraction (CBED) are not so large and have nearly the same phases as those of crystal structure factors (Tanaka & Lehmpfuhl, 1972). In the case of CBED, the influence of non-elastically scattered electrons is small, because a thin region of thickness less than *ca.* 1000 Å is examined and most of non-elastically scattered intensities can be removed by subtracting the intensity scattered just outside the sharp diffraction disc which is formed by an aperture-limiting convergent angle (Goodman & Lehmpfuhl, 1967). This situation is in contrast with the case of electron microscopy, where inelastically and quasi-elastically scattered electrons which fall within the objective aperture cannot be separated from elastically scattered electrons, but are recombined by the objective lens. Many-beam calculation with use of the values of the absorption factors obtained by CBED gives only slight contrast for the 180° domains, in contrast to that observed in the electron-microscopic image. This result

suggests that there is little difference in elastically scattered intensities between the 180° domains.

If we consider that the origin of the observed intensity difference in the electron-microscopic image is thermally scattered electrons passing through the objective aperture, all the results are explained reasonably. As TDS at small angles is considered to give poor interference (Takagi, 1958; Cundy, Howie & Valdré, 1969), it forms a diffuse background. Therefore the observed intensity difference of the diffuse background between the 180° domains is considered to be due to the difference in the TDS. The temperature dependence of the background (Fig. 3) is understood as follows. As the temperature rises the lattice vibrations which give the increase of the difference in background intensities are excited. As the temperature rises further toward the Curie point, the deviation of atoms from the centrosymmetric position decreases markedly. Thus, the difference in the background between the 00 $\bar{l}$  and 00 $l$  reflexions diminishes. The abnormal values evaluated for the absorption factors are the consequence of the application of the phenomenological dynamical theory to the intensities, including not only elastically scattered intensity but also quasi-elastically scattered intensity (TDS).

The difference in the background intensities in the cases of BaTiO<sub>3</sub> and KNbO<sub>3</sub> is also considered to be dependent on temperature, in view of the present results. However, the temperature dependence was not remarkable in these substances, even though the domain motion prevents accurate measurement of it, especially in BaTiO<sub>3</sub>. The inconspicuous temperature dependence is presumably attributed to the fact that enough contrast exists even at the lowest temperature in the tetragonal phase and that the tetragonal phase of the substances exists over a narrow temperature range.

According to the theory of first-order TDS the intensity ( $I_{\text{TDS}}$ ) is proportional to  $(\xi \cdot s)^2 / (v^2 \cdot q^2)$ , where  $\xi$ ,  $s$ ,  $v$  and  $q$  are the amplitude vector, the scattering vector, the frequency of the vibration and the vector from a reciprocal-lattice point respectively, so that,  $I_{\text{TDS}}(s) = I_{\text{TDS}}(\bar{s})$ . The intensity difference may be explained by introducing an imaginary potential or an odd-order anharmonic potential for lattice vibration, except that the origin of such potentials must be explained.

Preliminary intensity measurements of TDS from BaTiO<sub>3</sub> by the X-ray method do not show appreciable differences between  $I_{\text{TDS}}(s)$  and  $I_{\text{TDS}}(\bar{s})$ . This suggests that the observed intensity difference may be characteristic of electron-microscopic observation. If this is the case, the size effect of the specimen, the effect of electron irradiation in the ferroelectric crystals, *etc.* have to be studied. A detailed X-ray study is planned for the near future.

The author wishes to express his thanks to Dr K. Tsuzuki for supplying good single crystals of PbTiO<sub>3</sub>.

He also thanks Professor S. Hosoya and Mr T. Fukamachi for the measurement of TDS by X-ray diffraction. For the calculation part of the work, he is indebted to Professor K. Molière for the generous hospitality of his department and also thanks the Max-Planck-Gesellschaft and the Alexander von Humboldt-Stiftung for financial support.

#### References

- CUNDY, S. L., HOWIE, A. & VALDRÉ, U. (1969) *Phil. Mag.* **20**, 147–163.
- FUJIMOTO, F. (1959). *J. Phys. Soc. Japan*, **14**, 1558–1568.
- GEVERS, R., BLANK, H. & AMELINCKX, A. (1966). *Phys. Stat. Sol.* **13**, 449–465.
- GOODMAN, P. & LEHMPFUHL, G. (1967). *Acta Cryst.* **22**, 14–24.
- KOHRA, K. & WATANABE, H. (1961). *J. Phys. Soc. Japan*, **16**, 580–581.
- NIEHRS, H. (1959). *Z. Naturforsch.* **14A**, 504–511.
- POGANY, A. P. & TURNER, P. S. (1968). *Acta Cryst.* **A24**, 103–109.
- TAKAGI, S. (1958). *J. Phys. Soc. Japan*, **13**, 287–296.
- TANAKA, M. & HONJO, G. (1964). *J. Phys. Soc. Japan*, **19**, 954–970.
- TANAKA, M. & HONJO, G. (1966). *Sixth International Congress for Electron Microscopy, Kyoto*, pp. 83–84.
- TANAKA, M. & HONJO, G. (1970). *Seventh International Congress for Electron Microscopy, Grenoble*, pp. 55–56.
- TANAKA, M. & LEHMPFUHL, G. (1972). *Jap. J. Appl. Phys.* **11**, 1755–1756.
- TANAKA, M., YATSUHASHI, T. & HONJO, G. (1970). *J. Phys. Soc. Japan*, **28**, Suppl., 386–388.
- WICKS, B. J. & LEWIS, M. H. (1968). *Phys. Stat. Sol.* **26**, 571–576.

*Acta Cryst.* (1975). **A31**, 63

## Structure Analysis of the $\gamma$ Phase in the Vanadium Oxide System by Electron Diffraction Studies

BY B. ANDERSSON

*Department of Physics, University of Oslo, Oslo, Norway*

(Received 3 July 1974; accepted 7 August 1974)

The structure of the  $\gamma$  phase ( $\text{VO}_{0.53}$ ) has been analysed by electron diffraction from single crystals. Intensities in the spot patterns were compared with calculations based on dynamical theory for scattering of electrons for ideal crystals. It was found necessary to include corrections due to bending of the crystal. The structure can be regarded as a rock-salt type with oxygen vacancies or as body-centred cubic with interstitial oxygen. Possible ways of distributing oxygen on the available sites have been tried. The only structure models which produce a reasonable fit have oxygen atoms arranged in close-packed rows with the vanadium atoms displaced to give V–O and V–V distances in accordance with the corresponding distance in V and VO. Diffuse scattering indicating further ordering of vacancies has been observed.

### 1. Introduction

In the lower part of the composition range in the V–O system a phase, called  $\gamma$  in the nomenclature given by J. Stringer (1965), appears at the approximate composition  $\text{VO}_{0.5}$ . Its existence was first proposed by Rostoker & Yamamoto (1955) and was confirmed by a phase analysis by Westman & Nordmark (1960), based on X-ray powder diffraction. From a comparison with the neighbouring phases they suggested the structure to be a transition between the structure of the  $\beta$  phase ( $\text{VO}_{0.3}$ ) and the monoxide. Later, Westman (1963) proposed a monoclinic unit cell for indexing the line patterns. The composition range around  $\text{VO}_{0.5}$  has also been studied by electron microscopy combined with X-ray powder diffraction by Cambini, Pellegrini & Amelinckx (1971). They reported a phase at the same composition but proposed a different monoclinic unit

cell. Structure analysis of the  $\gamma$  phase has not been carried out so far.

Such an analysis is of interest also for the understanding of the nature and ordering of defects in the neighbouring suboxide and monoxide regions. A main aim of the present investigation, in which a structure analysis has been carried out by means of electron diffraction, has been to gain further insight into the defect structure in the lower part of the monoxide region. Since the single crystals are small, neutron or X-ray single-crystal methods could not be applied; neither could powder methods because the lines contain contributions from several non-equivalent reflexions.

The ease with which single-crystal patterns can be obtained by electron diffraction techniques, combined with the imaging of the diffracting regions, leads to easy determination of the unit cell and also of possible space groups. It is mainly this powerful side of the